Electronic Journal of Biotechnology 22 (2016) 81–89

HOSTED BY

Contents lists available at ScienceDirect

Electronic Journal of Biotechnology

Research Article

Production, purification and characterization of recombinant human antithrombin III by *Saccharomyces cerevisiae*

Maheswara Reddy Mallu, Sandeep Vemula, Srinivasa Reddy Ronda *

Department of Biotechnology, Centre for Bioprocess Technology, KLEF University, Guntur 522 502, Andhra Pradesh, India

ARTICLE INFO

Article history:
Received 14 September 2015
Accepted 13 May 2016
Available online 02 July 2016

Keywords:
Biological activity
Cell lysis
Cross flow filtration
Fed-batch fermentation
Purification
Secondary structure

ABSTRACT

Background: Antithrombin III (ATIII) is a protein that inhibits abnormal blood clots (or coagulation) by breaking down thrombin and factor Xa. ATIII helps to keep a healthy balance between hemorrhage and coagulation. The present work demonstrated the production, purification and characterization of recombinant human antithrombin (rhAT) from yeast *Saccharomyces cerevisiae* BY4741 was demonstrated. After expression of rhAT by *S. cerevisiae*, the biomass and rhAT concentration were analyzed through fed-batch fermentation process.
Results: In fed-batch fermentation, the biomass (maximum cell dry weight of 11.2 g/L) and rhAT concentration (312 mg/L) of the expressed rhAT were achieved at 84 h of cultivation time. The maximum cell lysis efficiency (99.89%) was found at 8 s sonication pulse and 7 mL lysis buffer volume. The rhAT protein solution was concentrated and partially purified using cross-flow filtration with the recovery yield and purity of 95 and 94%, respectively. The concentrated solution was further purified by the single step ion exchange chromatography with the recovery yield and purity of 55 and ≥98%, respectively. The purified rhAT was characterized by various analytical techniques, such as RP-HPLC, FT-IR, CD, SDS-PAGE, western blotting, and Liquid chromatography mass spectrometry (LC–MS) analysis. The biological activity of rhAT was analyzed as heparin cofactor to meet the therapeutic grade applications.
Conclusions: The simple, cost-effective and economically viable nature of the process used in the present study for the production of rhAT will be highly beneficial for the healthcare sector. This may also be used to produce other value-added therapeutic recombinant proteins expressed in *S. cerevisiae*, with greater effectiveness and ease.

1. Introduction

Antithrombin (AT) plays a central role in the regulation of blood coagulation and is the major physiological serine proteinase inhibitor that inactivates abundant proteinases in the case of blood coagulation cascade, mainly thrombin and factor Xa [1,2]. AT is a single-chain glycoprotein (432 amino acids, MW 58 kDa) with three disulfide bridges and four carbohydrate side chains linked at four asparagine residue sites asparagine residue sites (96, 135, 155, and 192), which account for 15% of the total mass [3,4]. It is usually present in human plasma at a level of 150 mg/L [5]. It also inactivates target proteinase by forming a 1:1 stoichiometric stable covalent complex with the reactive center arginine-393 of AT and reactive site serine residue of the proteinase [6]. The inhibitory activity of AT for thrombin is accelerated 1000 fold with the addition of heparin [7]. AT is also used in the therapeutic treatment of acute thrombotic episodes and prophylaxis during surgery and pregnancy in patients with AT shortage [8]. In humans, AT is produced by fractionation of plasma acquired from the blood donors [9]. Nevertheless, unreliable blood source causes the potential risk of contamination of the product by blood-borne pathogens. The production of AT by rDNA technology would address the concerns of contamination with blood-derived pathogens [10]. Hence, the industrial-scale production of recombinant human antithrombin (rhAT) is necessary.

Saccharomyces cerevisiae (yeast) has been extensively used as a capable host for the production of recombinant proteins. Yeast is usually preferred as a host over *Escherichia coli* because it is a eukaryote and is capable of carrying out post-translational modifications in order to achieve biological activity and secondary structure [11,12]. From a practical biotechnological point of view, *S. cerevisiae* has a long history of utilization in large-scale conventional industrial processes, and unlike *E. coli*, it lacks measurable endotoxins. Hence, it is regarded as safe (GRAS) organism for the production of industrial products [13].

* Corresponding author.
E-mail address: rsr@kluniversity.in (S.R. Ronda).
Peer review under responsibility of Pontificia Universidad Católica de Valparaíso.

http://dx.doi.org/10.1016/j.ejbt.2016.06.002

In general, different methods are used for the large-scale production of recombinant proteins from yeast. Batch and fed-batch fermentation processes are the state-of-the-art bioprocesses used for the production of industrial products. A fed-batch system enables us to control the addition of substrate for cell growth and product formation. This type of fermentation mode increases the cell density and extends the growth phase of cells compared to the batch fermentation process. In the fed-batch fermentation, the heterologous porcine insulin precursor concentration has been reported to reach five times the level obtained in the shake flask fermentation process [14].

In the present work, a study has been conducted on batch and fed-batch fermentation processes to analyze biomass and yield of rhAT using *S. cerevisiae* BY4741.

2. Materials and methods

2.1. Production of rhAT in a bioreactor

The recombinant *S. cerevisiae* BY4741 was cultivated in two modes of fermentation processes, i.e., batch and fed-batch fermentation, in a 5 L bioreactor (Minifors, Infors HT, Switzerland) with a working volume of 3 L. The *S. cerevisiae* minimal media consisted of 0.67% yeast nitrogen base (YNB) without uracil (HiMedia), 0.192% drop out powder (complete supplement mixture: aspartic acid, histidine, isoleucine, methionine, phenylalanine, proline, serine, tyrosine, and valine), and 2% carbon source (dextrose or raffinose). The bioreactor was inoculated with 500 mL of a 30 h pre-culture. Batch fermentation was started for initial cell growth. After depletion of the initial carbon source in the batch medium, the feeding was carried out to allow the cell mass concentration to increase exponentially. After a certain time (24 h), the fed-batch process was initiated by the addition of feed consisting of 20% galactose and 10% raffinose at regular time intervals (10 mL/2 h). The saturated sterile air inside the reactor was maintained with a condenser, and the pH was analyzed with a Mettler Toledo (Bedford, MA, USA) glass electrode, which was maintained at 7.1 ± 0.2 by the addition of 5 N sodium hydroxide and 3 N phosphoric acid solutions. The dissolved oxygen (DO) was measured by a Hamilton sensor (Bonaduz AG, GR, Switzerland). Aeration was provided using a sterile filter air (0.2 μ), which was operated at 2.0 vvm, and the agitation was maintained at 250 rpm.

2.2. Cell disruption

The fermented broth was harvested, and the pellet was collected by centrifugation (Sorvall ST 16 R, Thermo scientific, USA) at 4°C, 40,000 × g for 15 min. The weight of the pellet was calculated as dry cell weight (DCW, g/L). The cells were washed with wash buffer containing 0.05 M ethylenediaminetetraacetic acid (EDTA) (pH 8.0) and 0.01 M Tris–HCl (pH 7.6). The cells were then lysed by sonication (20 kHz, for 2–4 time intervals) and frequent homogenization using lysis buffer containing 0.01 M Tris–HCl (pH 7.6), 1% dimethylsulfoxide (DMSO), 50 mM NaCl,1 mM EDTA, 0.5% sucrose, and 1 mM phenylmethylsulfonyl fluoride (PMSF). A very low concentration of NaCl was used in the lysis buffer since the purification process involved ion exchange chromatography (IEC). The cell lysis procedure was optimized by employing various sonication pulses and lysis solution volumes at constant pellet weight of 1 g.

2.3. Analysis of biomass and rhAT concentration during fermentation

The post-induced culture samples (5 mL) were taken at 12 h intervals for 84 h, and the total cell concentration was determined by measuring the optical density at 600 nm (OD_{600}) using a UV–Vis spectrophotometer (Halo DB-20, Dynamica, Australia). The samples were considered to be diluted if the absorbance was above 0.5. The cells were collected by centrifugation at 35,000 × g for 10 min, the supernatant was discarded, and the DCW was calculated in triplicates.

The concentration of rhAT in the cell lysate solution during fed-batch fermentation was estimated by reverse phase liquid chromatography (RP-HPLC) (Shimadzu, Japan) [15]. The concentration of the rhAT was determined using the rhAT reference standard curve.

2.4. Concentration and partial purification by cross-flow filtration system

The protein solution (lysate) was concentrated and clarified using cross flow-filtration (CFF) system (Quix stand, GE Healthcare Life sciences, Sweden) through a constant volume of 500 mL. The protein solution was concentrated using a 30 kDa hollow fiber molecular weight cut-off (MWCO) cartridge (GE Healthcare Bioscience Corp, USA) with nominal flow path length of 30 cm and a cross-sectional area of 650 cm^2. The protein under CFF is mainly affected by temperature and transmembrane pressure. Hence, the filtration efficiency of rhAT protein solution was optimized by adopting various ranges of temperature (18, 22 and 26°C) and transmembrane pressure (12, 16 and 20 psi) [16].

2.5. Purification strategies of rhAT

The impure mixture of rhAT is subjected to the IEC step. The fast protein liquid chromatography system (FPLC), AKTA Prime plus (GE Healthcare Life sciences, Uppsala, Sweden) was used for the purification of rhAT from the cross flow filtered sample. The size exclusion chromatography (SEC) (Sephadex G-200) followed by IEC (SP-Sepharose FF) was performed with Bioprocess glass column (BPG) XK16/20 and packed with 30 mL of the matrix. The column flow rate and temperature were maintained at 2 mL/min and 20°C, respectively, throughout the process. The sodium phosphate buffer (25 mM) at pH 5.4 was used to equilibrate the stationary phase, and the protein sample was directly loaded onto the column with the same flow rate. The elution buffer with 25 mM sodium phosphate, pH 5.4 and 0.5 M NaCl was used to elute rhAT from the column.

2.6. RP-HPLC analysis

RP-HPLC was performed to analyze the qualitative properties of rhAT. An HPLC system (Shimadzu, Kyoto, Japan) was fitted with LC Prominence SPD 20A UV–Visible detector and LC 20 AT binary pumps. The analysis of rhAT was carried out at the following conditions: flow rate 1.0 mL/min, wavelength 280 nm, pressure 80 Kgf and controlled temperature 40°C. The C18 5 μ column (250 × 4.6 mm) (Phenomenex, USA) was used for rhAT analysis. The mobile phase A consisted of water: acetonitrile (87.5:12.5 v/v) with 0.1% trifluoroacetic acid (TFA), and the mobile phase B consisted of water: acetonitrile (30:70 v/v) with 0.08% TFA as an ion pairing agent. The rhAT was eluted using linear gradient mode with 5% B to 90% B in 20 min and 90% B to 5% B in 40 min. The injection volume was 20 μL for all the runs, and rhAT (National Institute for Biological Standards and Control-NIBSC, UK) was used as a reference standard. All the chromatograms were stabilized with the major peak, and a chromatogram analysis was executed through the LC Solution software.

2.7. Secondary structure analysis

The secondary structure of rhAT was characterized by circular dichroism (CD) and Fourier transform-infrared (FT-IR) spectroscopy. The CD spectra of purified rhAT were evaluated using the AVIV 420SF spectropolarimeter (Lakewood, NJ, USA) that was fixed to a thermostated cell holder and a thermostatic water bath with a 20 nm/min scan speed. The cylindrical cells of high optical quality (Optical Cell, Woodbine, MD) with a path length of 2 cm were used to record the spectra and reported the average of five consecutive scans. All the experiments were carried out at 24°C. The rhAT spectra

were recorded from the scan range of 250 to 310 nm using a 2 mm path length quartz cell with a sensitivity of 1 mdeg per cm.

The purified rhAT secondary structure was also assessed by FT-IR spectroscopy. FT-IR, Spectrum Two™ (Perkin Elmer, USA) with Lithium tantalite (LiTa03) infrared detector was used to measure the rhAT samples. Hygroscopic calcium fluoride (CaF_2) glass windows with 4 μ path length spacer were used to analyze the rhAT samples. The spectra were achieved from the scan range of 4000 to 450 cm^{-1} in transmission mode with 32 cm^{-1} resolution. The best spectra were acquired by performing 100 scans with a scan speed of 2 cm^{-1}. All the spectra were smoothed and deconvoluted using Spectrum 10™ software.

2.8. SDS-PAGE and western blot analysis

The purity of rhAT was analyzed by SDS-PAGE and western blotting analysis. A 12% acrylamide SDS gel was achieved using the Mini protean II system (Bio-Rad Inc., CA, USA). Due to the high molecular weight of AT (58 kDa), the gel was run at a stable 50 V for 4 h to get the clear separation of bands with a high resolution. After the separation of the bands, the gel was stained with comassie brilliant blue (CBB) R-250 overnight. After gel electrophoresis, the rhAT protein was moved onto polyvinylidene difluoride (PVDF) membrane at an invariable voltage of 50 V for 1 h. The membrane was incubated with blocking buffer containing 5% skim milk powder and phosphate buffer saline (PBS) for 1 h at room temperature. It was then incubated with the polyclonal antibody (1:1000) generated from the rabbits for 80 min at 28°C. The membrane was washed with PBS containing 0.1% Tween 20 and incubated with horseradish peroxidase (HRPO)-conjugated goat IgG antibody (Bio-Rad Inc., USA) for 40 min at 28°C. The membrane was again washed with buffer containing 10 mM Tris (pH 8.0) and 0.5 M sodium chloride and subsequently incubated with a chromogenic substrate solution (Thermo Fisher Scientific, USA).

2.9. Liquid chromatography–mass spectrometry (LC–MS) analysis

Prior to the injection of the sample, the purified rhAT was diluted five-fold with formic acid (0.1%) in water. All the experiments were carried out using an Agilent 1290 UHPLC system that is equipped with a quaternary pump, vacuum degasser, thermostated well-plate auto sampler, column oven, and C18 column (Waters, Milford, USA) joined to an Agilent 6520 QTOF LC/MS mass spectrometer with a binary-nebulizer. Mobile phase A (0.1% aqueous formic acid) and mobile phase B (acetonitrile with 0.1% formic acid) were used as solvents, and 5% B was used during initial conditions at constant column temperature and flow rate. The optimal flow rate and temperature were estimated experimentally to be 0.5 mL/min and 50°C, respectively. The gradient program was used as follows: 0–1 min 5% B, 1–6 min 80% B, 6–8 min 95% B, and 8–10 min 5% B. The mass spectra of rhAT were analyzed with the following QTOF/source parameters: Nebulizer: 25 psig; Drying Gas: 10 L/min at 300°C; Sheath gas: 10 L/min at 400°C; VCap: 3000 V; Fragmentor: 100 V; MS Scan: 100–3200 m/z at 2 spectra/s (Intact Mass); Skimmer: 60 V OCT 1RF; and Vpp: 750 V.

2.10. Biological activity of rhAT

The biological potency of the purified rhAT was estimated as a heparin cofactor (HC) activity with a commercially available kit, which utilizes the thrombin specific-chromogenic substrate S-2238 (Testzym antithrombin III 2 assay kit; Daiichi Pure Chemical, Tokyo) [10].

2.11. Statistical analysis

Statistical analysis was conducted using Graph pad In Stat 3.0. The experiments for protein recovery, purity and bioactivity were conducted in triplicates of experimentation, and the mean values with standard deviations (SD) were also recorded.

3. Results and discussion

3.1. Production of rhAT in the bioreactor

When a high cell density is the primary concern, the fed-batch cultivation is more useful for the biomass and product formation because the protein expression is in proportion to the cell density

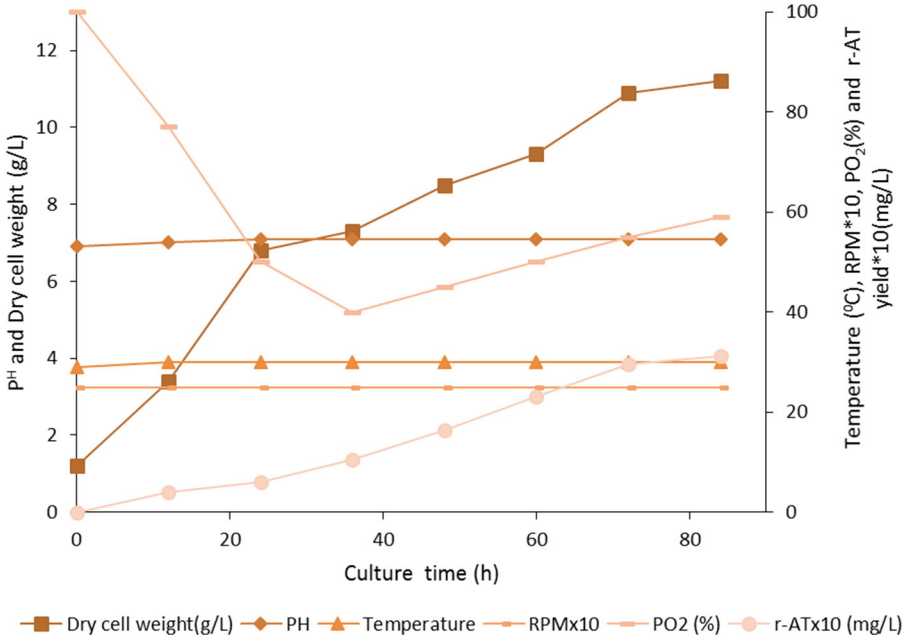

Fig. 1. Fed-batch fermentation process variables of rhAT from *Saccharomyces cerevisiae* BY4741. Initially, the process was operated in batch mode up to 24 h, and the fed-batch process was ended at 84 h. The addition of limiting substrate was started at 6.8 g/L dry cell weight, and the maximum biomass yield (11.2 g/L) and rhAT concentration (312 mg/L) were observed at 84 h. The process variables such as rpm and rhAT concentration values were multiplied with 10 according to their relevant axis values.

Table 1
Effect of sonication pulses and lysis buffer volumes on cell lysis. The resulting analysis represents mean values with SD of three repeated experiments.

Parameter		Cell lysis efficiency[a] (%)
Sonication pulse (s)	2	98.94 ± 0.02
	4	99.20 ± 0.03
	6	99.34 ± 0.02
	8	99.57 ± 0.04
	10	99.52 ± 0.02
Lysis buffer volume (mL)	3	99.68 ± 0.03
	5	99.76 ± 0.02
	7	99.89 ± 0.02
	10	98.59 ± 0.03

[a] The cell lysate solution was serially diluted with 0.85 M NaCl solution and separately spread on the YNB-agar plates with ampicillin.

[17,18,19]. The rhAT was produced by *S. cerevisiae* using the batch and the fed-batch fermentation process. The fed-batch fermentation profile of rhAT production is illustrated in Fig. 1. It can be seen that the maximum CDW and rhAT concentration were achieved (11.2 and 312 mg/L, respectively) at 84 h of fermentation process. The overall productivity of rhAT was significantly superior to that of the previously reported research [20]. The increase in the overall productivity could be due to the moderate specific growth rate by the addition of feed at controlled conditions during fed-batch cultivation. Initially, the oxygen uptake rate (OUR) was found to be 100% air saturation that showed a gradual decrease in the dissolved oxygen concentration (pO2). It was observed that the dissolved oxygen concentration (40%) at 36 h indicated the presence of exponential phase cells with a high specific growth rate. The increase in pO2 was observed progressively, which indicated that the cells reached a stationary or decline phase. During fermentation, the pO2 was maintained at 40% and above to reduce the aggregation of toxic compounds within the cells. The presented fed-batch process was confirmed to be a suitable mode of fermentation for the large-scale production of rhAT.

3.2. Cell lysis analysis

After production, the cells were disrupted by frequent homogenization and sonication processes. To achieve maximum rhAT recovery, the lysis protocol was optimized by employing various strategies, such as i) different sonication pulses (2, 4, 6, 8 and 10 s) and ii) different buffer volumes (3, 5, 7 and 10 mL). The cell lysate solution was serially diluted with 0.85 M NaCl solution and separately spread on the YNB-agar plates with ampicillin. The cell lysis efficiency was analyzed based on the cell counting. Table 1 describes the cell lysis efficiency with adopted conditions. It can be observed that the maximum cell lysis efficiency (99.57%) was achieved with 8 s sonication pulse, whereas the lowest efficiency (98.94%) was observed with 2 s sonication pulse.

On the other hand, the highest cell lysis efficiency (99.89%) was achieved with the buffer volume of 7 mL, and the lowest efficiency (99.68%) was observed with 3 mL of buffer volume (Table 1). From these results, it was clearly observed that buffer volumes should not be too low or too high, and it must be optimum to achieve maximum cell lysis efficiency.

Table 2
The effect of lysis buffer volumes on purified and control antithrombin with respect to 5 and 10 mL lysis buffer volumes. Similar profile of both purified and control antithrombin activity was observed with 5 and 10 mL lysis buffer volumes. The resulting analysis represents mean values with SD of three repeated experiments.

Lysis buffer volume (mL) with fixed concentration of AT (0.35 mg/mL)	Purified rhAT activity as HC activity (IU/L)	Control AT activity as HC activity (IU/L)
5	365.7 ± 0.1	366.7 ± 0.1
10	365.3 ± 0.1	366.2 ± 0.1

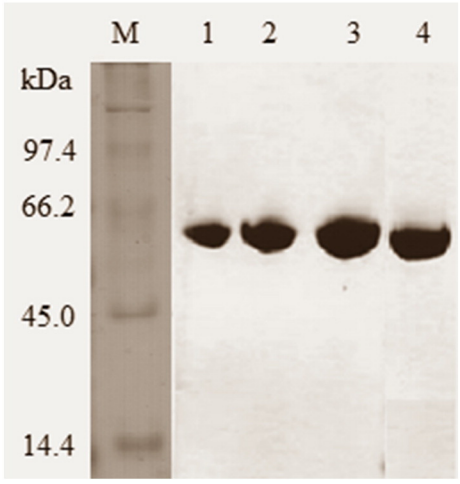

Fig. 2. Native PAGE analysis of rhAT lysate samples with 5 and 10 mL of lysis buffer. Lanes 1 and 2 show the rhAT test samples. Lanes 3 and 4 show control AT samples. Similar antithrombin (58 kDa) bands were observed with respect to different volumes of lysis buffer volumes (5 and 10 mL) and the molecular weight of both purified and control antithrombin (58 kDa) was compared with molecular weight marker (lane M).

However, to know the effect of lysis buffer volume on rhAT activity, the cell lysate samples with 5 and 10 mL lysis buffer were subjected to centrifugation and followed by purification (CFF and SEC with Sephadex G-200). After purification, rhAT activity was analyzed as HC activity through chromogenic assay (TESTZYM ATIII 2 kit; Daiichi Pure Chemical, Tokyo) with the fixed concentration of purified rhAT (0.35 mg/mL). On the other hand, the effect of lysis buffer volume (5 and 10 mL) was also analyzed on control AT activity with the fixed concentration of control AT (0.35 mg/mL). From the experimental results (Table 2), it can be observed that no much variation in the activity of both purified and control AT with respect to two different volumes of lysis buffer (5 and 10 mL). The native PAGE gel (Fig. 2) was also performed to check the both purified and control AT activity. From the experimental observations, it has clearly observed that cell lysis efficiency was affected by variation in lysis buffer volume but not AT activity and its stability.

3.3. Concentration and partial purification

CFF is an efficient process of concentration and partial purification of protein solutions without any loss of proteins and their activity. The primary concentration and purification of recombinant protein are essential to prepare a clarified feed stream for the final purification step [21]. Various recombinant proteins such as recombinant human granulocyte colony stimulating factor (rhG-CSF) and monoclonal antibodies have been successfully concentrated using the CFF system with >95% purity [16,22]. In the present work, an investigation has been conducted to analyze the effect of temperature (18, 22 and 26°C)

Table 3
Effect of temperature and transmembrane pressure on rhAT filtration efficiency. The result analysis was performed in triplicates with mean values of SD.

Physical parameter		RPM	V_o (mL)	V_p (mL)	V_r (mL)	C_f	T (min)	Yield (%)	Purity (%)
Temperature (°C)	18	350	500	410	90	5.55	91	80 ± 1.2	91
	22	350	500	454	46	10.86	74	92 ± 1.6	96
	26	350	500	421	79	6.32	82	74 ± 1.4	93
Transmembrane pressure (Psi)	12	350	300	218	82	3.65	65	75 ± 1.5	90
	16	350	300	256	44	6.81	48	95 ± 1.3	94
	20	350	300	230	70	4.28	57	81 ± 1.2	88

V_o = initial volume; V_p = permeate volume; V_r = retantate volume; C_f = concentration factor is the ratio of the feed volume to the final volume; T = total time (min).

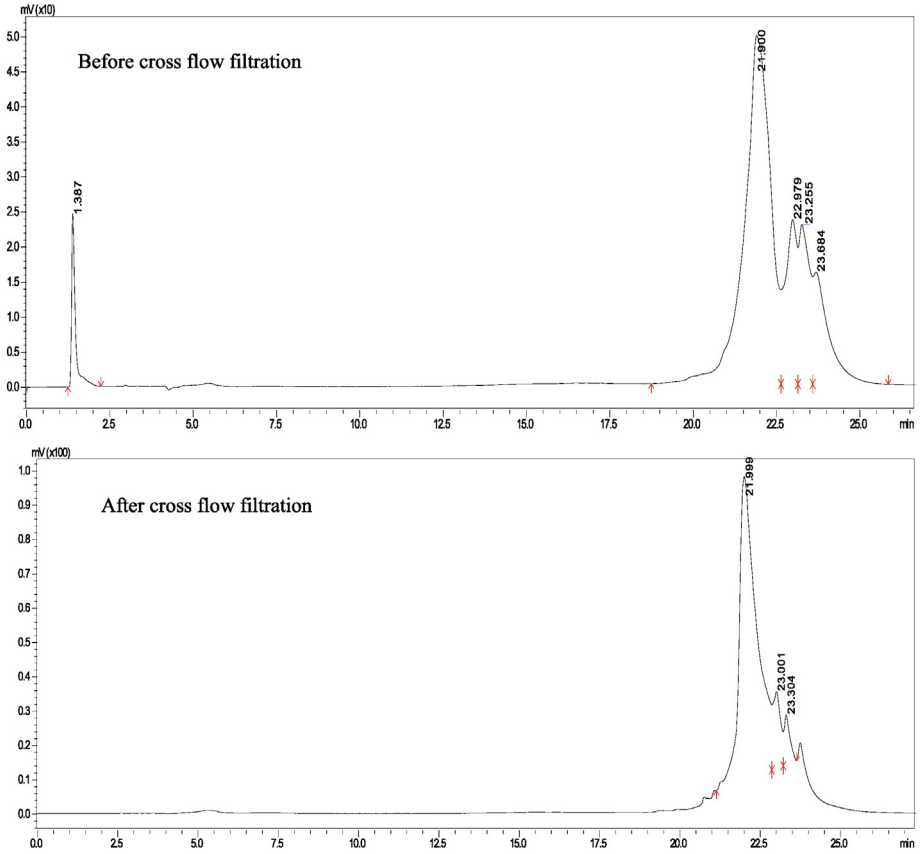

Fig. 3. RP-HPLC profiles of cell lysate before and after cross flow filtration. The maximum purity of rhAT (≥94%) was achieved with temperature (22°C) and transmembrane pressure (16 psi).

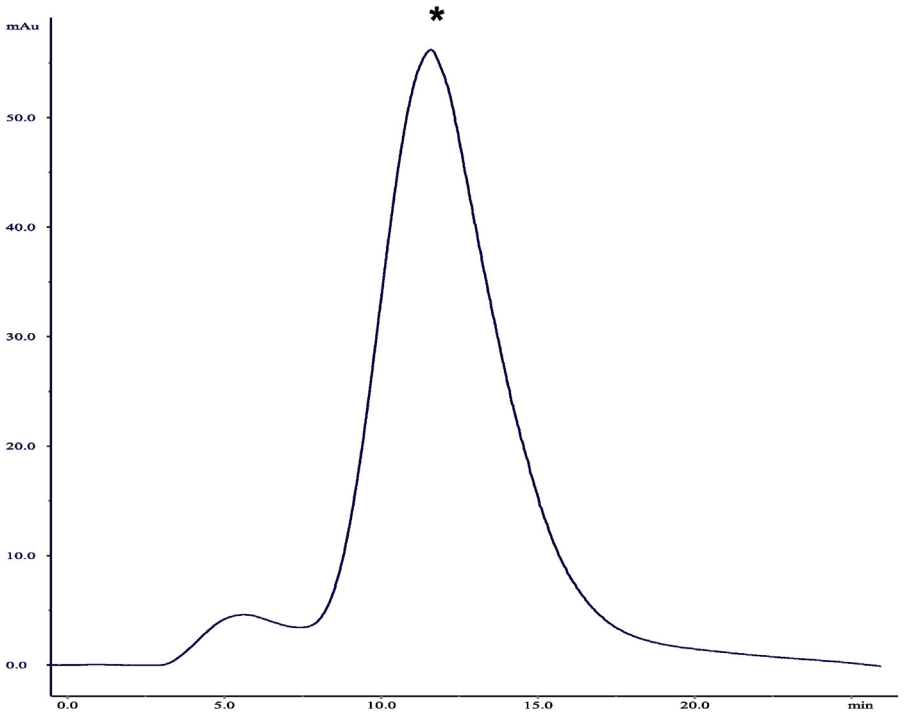

Fig. 4. FPLC chromatogram of rhAT eluted through the IEC with SP-Sepharose FF resin. Monomer peak (indicated with *) of rhAT with a good resolution was separated with maximum recovery yield and purity of 55 and ≥98%, respectively.

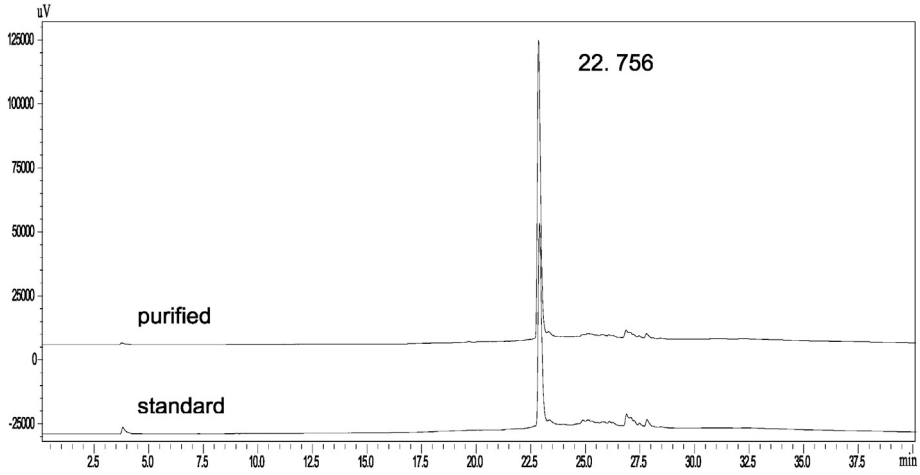

Fig. 5. RP-HPLC analysis of purified rhAT eluted through a phenomenex C-18 column (250 × 4.6 mm) column. The peaks were auto scaled according to the largest intensity peak. The maximum purity of the rhAT (≥98%) was observed with retention time 22.756 min.

and transmembrane pressure (12, 16 and 20 psi) on the clarification and concentration of rhAT protein solution using CFF. Table 3 shows the filtration efficacy of rhAT solution. The maximum yield (92%) of rhAT was observed at 22°C with 96% purity and 10.86 concentration factor. On the other hand, it can be seen that the 16 psi transmembrane pressure was suitable for the filtration of rhAT with the yield, purity and concentration factor of 95%, 94% and 6.81, respectively (Table 3). However, the cell lysate consisted of a mixture of various proteins, proteins below 30 kDa, cell contaminants like nucleic acids, DNA, lipopolysaccharides and other cellular components that moved freely across the permeable membrane. Fig. 3 shows the RP-HPLC profiles of rhAT before and after CFF. It can be seen that before CFF, the contaminant's population was assimilated with rhAT protein. After CFF, the generation of concentrated and partially purified protein was eluted from the column, and the obtained HPLC chromatogram indicated a single major peak with fewer impurities.

3.4. Purification of rhAT

The objective of a purification process is not only the removal of unnecessary contaminants but also the increase in the concentration of the target protein and its transfer to an environment, where it remains stable and ready for the intended application. However, if the protein is intended towards therapeutic use, it must be extremely pure. The purification must be done in minimum steps to get an inexpensive drug with a higher degree of purity [23]. Even though, the heparin affinity columns are available in the market, simple and cost-effective size exclusion and ion exchange resins were used from the economic perspective. This can be achieved by choosing the right combination of purification technique. In the present study, the concentrated and partially purified rhAT solution was subjected to SEC followed by IEC. Fig. 4 shows the FPLC chromatogram of rhAT protein eluted from the SP-sepharose FF ion exchange column. From the

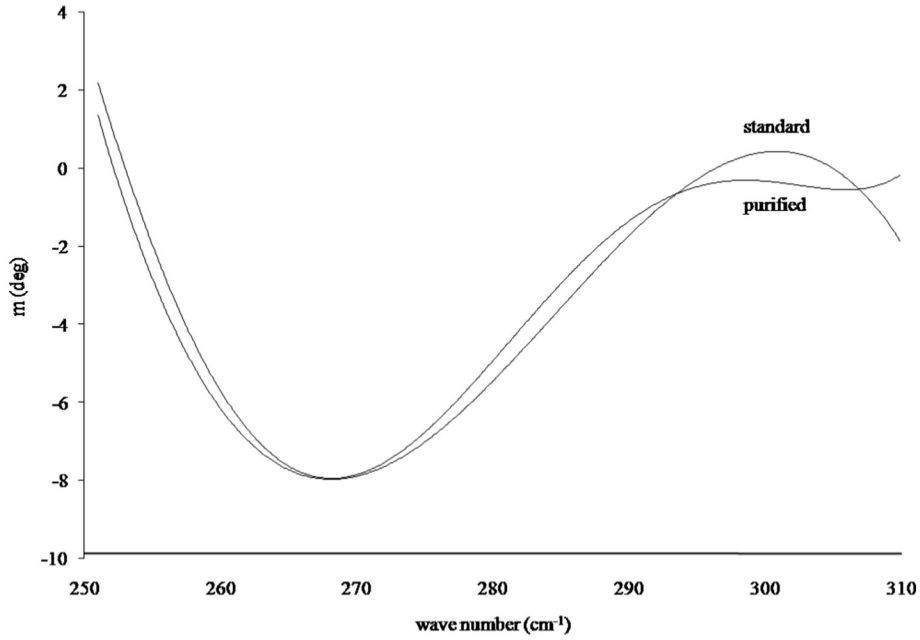

Fig. 6. Secondary structure analysis of rhAT by CD spectroscopy. The CD spectra of both the standard and purified rhAT were shown as α-helix (32%), β-sheet (16%), beta turns (10%), and random coil form (6%) of polypeptide chain components.

results, it can be seen that the single monomer rhAT peak was clearly separated from its dimer. AT was purified with SEC followed by IEC and conformed to be the monomeric form of rhAT. The same was revealed and confirmed by RP-HPLC analysis, which is considered to be sensitive than the PAGE analysis. The monomer peak fraction was collected at a volume of 10 mL with a concentration of 0.5 mg/mL. The maximum recovery yield and purity achieved with this step were 55 and ≥98%, respectively. In the present study, significant recovery yield and purity profiles of rhAT were achieved with IEC followed by SEC resins similar to that of heparin affinity columns.

3.5. Characterization of rhAT

The therapeutic molecules produced by r-DNA technology are extremely complex as compared to the chemically synthesized active ingredients. The recombinant-based therapeutic proteins show a higher structural heterogeneity and are subject to a range of enzymatic or chemical alterations. This protein heterogeneity results from the sequence variations generated from the proteolysis or transcriptional/translational errors from post-translational modifications, and from the degradation of products, which are formed through processing and final product storage. For that reason, the characterization and responsive analytical techniques are compulsory to assure the safety, quality and efficacy of the therapeutic protein products [24]. In the present study, the purified rhAT was characterized using various analytical techniques.

The purity of the rhAT was analyzed by RP-HPLC. Fig. 5 shows the RP-HPLC chromatogram of rhAT eluted from the IEC. A single symmetrical peak was obtained, indicating that it contains a homogeneous population of rhAT conformer with >98% purity, and it was correlated with the reference to standard rhAT.

The secondary structure of the rhAT was analyzed by the CD and FT-IR spectroscopy. Fig. 6 shows the structural assessment of rhAT. The presence of α-helix (32%), β-sheet (16%), β-turns (10%), and random coil form (6%) of polypeptide chain components with the rest

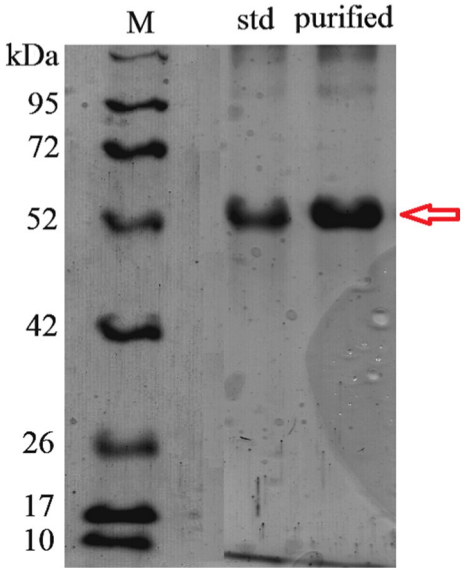

Fig. 8. SDS-PAGE analysis of purified rhAT. Lane M protein molecular weight marker, lane 1 rhAT reference standard and, lane 2 purified rhAT.

of the molecule were found to be in unordered form confirming its secondary structure, which is in conformity to earlier research [25].

The secondary structure of rhAT was also scrutinized by FT-IR spectroscopy. The second derivative structure of rhAT was correlated with reference standard rhAT. Fig. 7 shows the second derivative of rhAT curve-fitting IR spectra that were compared with a reference standard (NIBSC, UK). The major spectral variations were viewed in amide I and amide II due to the possibility of C═O stretching vibrations (1632 ± 2 cm^{-1}) and N—H deformation or bending (1620 ± 2 cm^{-1}) of amides attached with both the purified and standard rhAT proteins, respectively. The major spectral vibrations

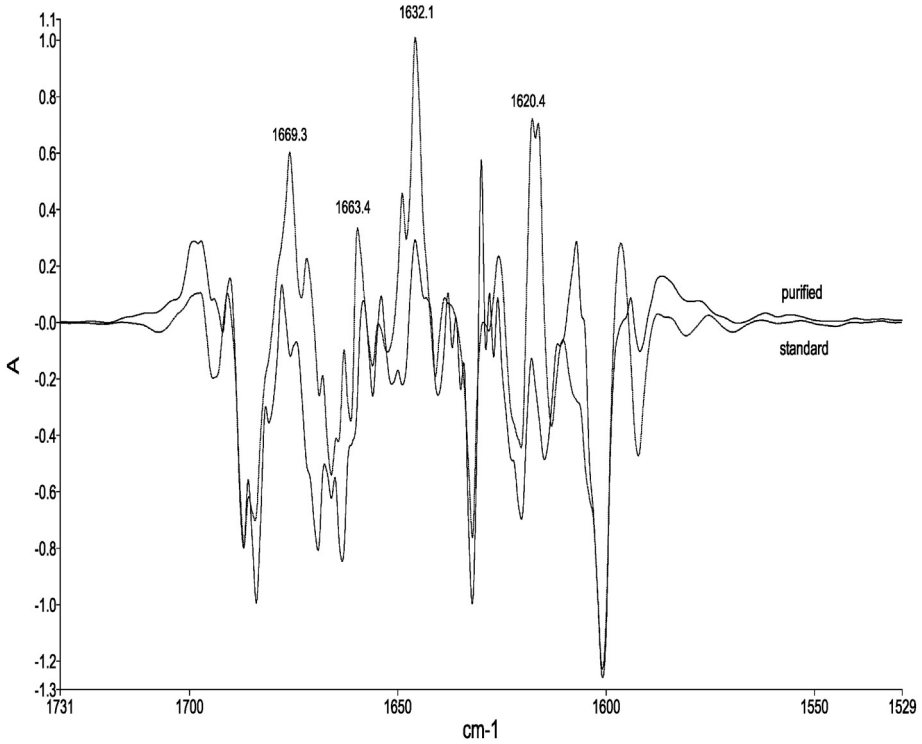

Fig. 7. FT-IR absorbance spectra of the purified and reference standard rhAT. Spectra shows the amide I and II bands, which are the backbone of the protein polypeptide chain. The secondary structural components of amide I region consists of α-helix (1663 ± 2 cm^{-1}) and β-sheet (1669 ± 2 cm^{-1}).

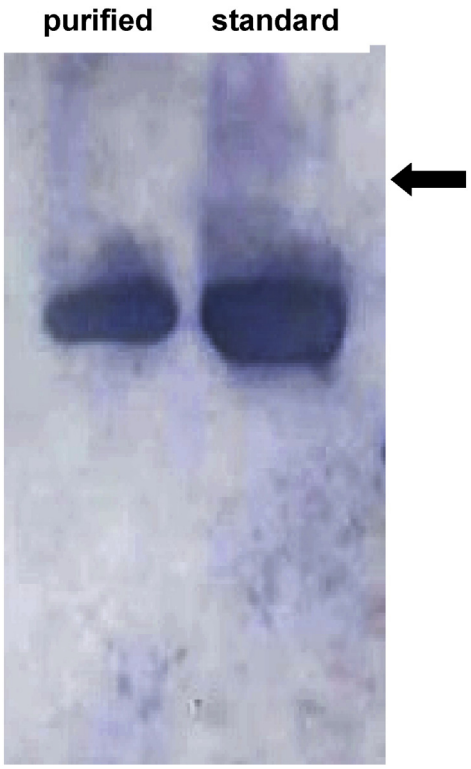

Fig. 9. Western blot analysis of the purified rhAT with a reference standard. Lane 1 shows the purified rhAT. Lane 2 shows standard rhAT. Western blot analysis of rhAT was performed using polyclonal antibody generated from the rabbits and horseradish peroxidase (HRPO)-conjugated goat anti rabbit IgG antibody.

were commonly monitored in both the proteins that confirmed its analogous nature towards each other along with similar absorption bands. It was also observed that, in both proteins, the amide I region represented the secondary structure study by showing the structural constituents such as α-helix (1663 ± 2 cm^{-1}) and β-sheet (1669 ± 2 cm^{-1}). The above studies are a good evidence for the secondary structure analysis of the rhAT as contrasted with the reference standard with 98% correlation.

The purified rhAT protein was also analyzed by SDS–PAGE and western blotting. Fig. 8 shows SDS-PAGE analysis of rhAT. A single target rhAT band confirmed the similarity between molecular mass (58 kDa) and the pattern exhibited with the standard (NIBSC, UK). After SDS-PAGE analysis, the gel was transferred to PVDF membrane by the electro blotting method. The transformation was immunodetected with rhAT antibodies (Invitrogen Antibodies Fisher Scientific), and a single band indicated the presence of rhAT, which was similar to

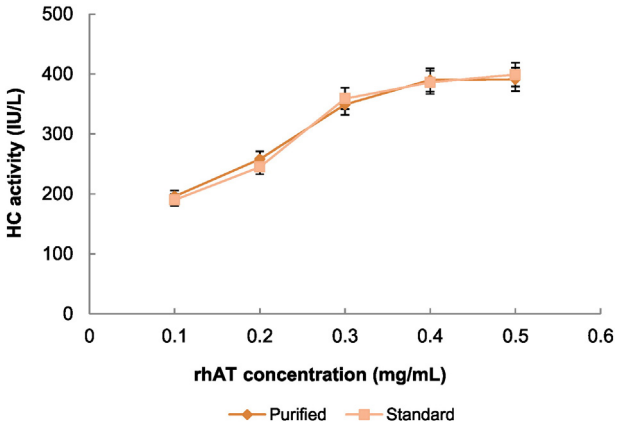

Fig. 11. Biological potency of rhAT by Testzym antithrombin III 2 assay kit (Daiichi Pure Chemical, Tokyo). A comparison profile of purified and reference standard of rhAT activity against various rhAT concentrations were presented. Biological activity profiles of both purified and reference standard showed significant correlation. All the experiments were performed in triplicates with mean ± standard deviation ($P < 0.005$).

the reference standard (Fig. 9). Fig. 10 shows LC–MS analysis of rhAT. The molecular mass of the rhAT was estimated to be 57,995 Da, which was close to the theoretical mass of 58 kDa.

The purified rhAT was diluted with 100 mM 2-amino-2-hydroxymethyl-1, 3-propanediol containing methylamine hydrochloride with pH 7.5 to make various concentrations of rhAT (0.1, 0.2, 0.3, 0.4 and 0.5 mg/mL). The rhAT samples with different concentrations were added to the mixture of thrombin and heparin (Testzym antithrombin III 2 assay kit; Daiichi Pure Chemical, Tokyo) before the commencement of the reaction by adding chromogenic S-2238 (1.43 g/L) substrate. After 5 min, the reaction was terminated by adding the citric acid solution. The reaction optical density at 405 nm was estimated by spectrophotometry. Fig. 11 shows the rhAT activity against various concentrations. From the results, it can be observed that an increase in the biological activity of rhAT as heparin cofactor activity was observed with increased rhAT concentration. The results were in accordance with the reference standard.

4. Concluding remarks

The fed-batch fermentation strategy described in the present study is trouble-free, highly successful, and reproducible. The CDW (g/L) and rhAT concentration were analyzed during the fed-batch fermentation process that exhibited maximum value of 11.2 g/L and 312 mg/L, respectively. The operation of fed-batch fermentation at a controlled specific growth rate of *S. cerevisiae* through galactose and raffinose feeding extended the duration of the batch time and

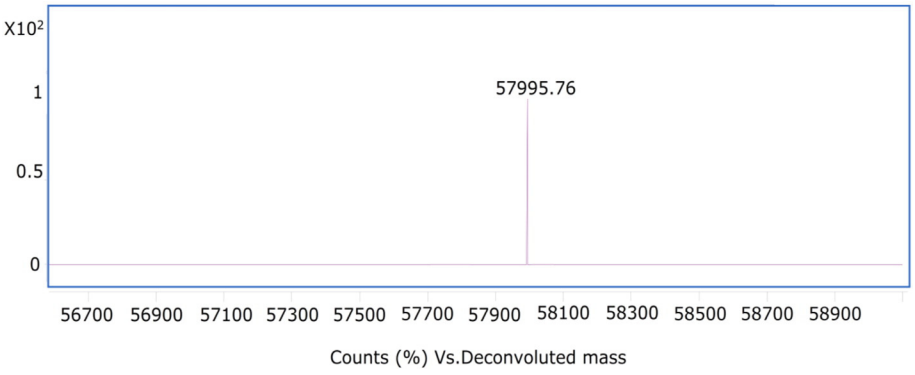

Fig. 10. LC–MS analysis of rhAT. Molecular mass of rhAT (57,995.36 Da) was matched with the antithrombin molecular weight, which is confirmed by the Bioconfirm software.

hence, was seen to affect the productivity of rhAT. With 8 s sonication pulses and 7 mL buffer volume of cell lysis protocol, the maximum cell lysis efficiency was found to be 99.89%. The lysate protein solution was concentrated and partially purified by CFF with the recovery yield and purity of 95 and 94%, respectively. Subsequently, it was finally purified by IEC method with the recovery yield and purity of 55 and ≥98%, respectively. The structural components of the amide I vibration, assessed by CD and FT-IR spectroscopy, revealed the alpha and beta helix structures that presented strong evidence for its secondary structural confirmation of rhAT. The purified rhAT underwent molecular mass (57,995 Da) analysis by LC/MS analysis. Finally, an increase in the biological activity of rhAT was observed with increased rhAT concentration and which is very close to the reference standard.

Conflict of interest

The authors declare no conflict of interest.

Acknowledgments

The authors are thankful to the management of KLEF University (KLU/IFR/615) for providing financial and laboratory support to carry out the present research work.

References

[1] Damus PS, Hicks M, Rosenberg RD. Anticoagulant action of heparin. Nature 1973; 246:355–7. http://dx.doi.org/10.1038/246355a0.
[2] Travis J, Salvesen GS. Human plasma proteinase inhibitors. Annu Rev Biochem 1983; 52:655–709. http://dx.doi.org/10.1146/annurev.bi.52.070183.003255.
[3] Hirose M, Kameyama S, Ohi H. Characterization of N-linked oligosaccharides attached to recombinant human antithrombin expressed in the yeast *Pichia pastoris*. Yeast 2002;19:1191–202. http://dx.doi.org/10.1002/yea.914.
[4] Schröder M, Körner C, Friedl P. Quantitative analysis of transcription and translation in gene amplified Chinese hamster ovary cells on the basis of a kinetic model. Cytotechnology 1999;29:93–102. http://dx.doi.org/10.1023/A:1008077603328.
[5] Murano G, Williams L, Miller-Andersson M, Aronson DL, King C. Some properties of antithrombin-III and its concentration in human plasma. Thromb Res 1980;18: 259–62. http://dx.doi.org/10.1016/0049-3848(80)90190-5.
[6] Olson ST, Richard B, Izaguirre G, Schedin-Weiss S, Gettins PGW. Molecular mechanisms of antithrombin-heparin regulation of blood clotting proteinases. A paradigm for understanding proteinase regulation by serpin family protein proteinase inhibitors. Biochimie 2010;92:1587–96. http://dx.doi.org/10.1016/j.biochi.2010.05.011.
[7] Kovacs B, Bereczky Z, Olah Z, Gindele R, Kerenyi A, Selmeczi A, et al. The superiority of anti-FXa assay over anti-FIIa assay in detecting heparin-binding site antithrombin deficiency. Am J Clin Pathol 2013;140:675–9. http://dx.doi.org/10.1309/AJCPVY4Z9XZMFOTH.
[8] Patnaik MM, Moll S. Inherited antithrombin deficiency: A review. Haemophilia 2008;14:1229–39. http://dx.doi.org/10.1111/j.1365-2516.2008.01830.x.
[9] Liumbruno G, Bennardello F, Lattanzio A, Piccoli P, Rosysetti G. Recommendations for the use of antithrombin concentrates and prothrombin complex concentrates. Blood Transfus 2009;7:325–34. http://dx.doi.org/10.2450/2009.0116-09.
[10] Kuwae S, Ohyama M, Ohya T, Ohi H, Kobayashi K. Production of recombinant human antithrombin by *Pichia pastoris*. J Biosci Bioeng 2005;99:264–71. http://dx.doi.org/10.1263/jbb.99.264.
[11] Kwon KS, Song M, Yu MH. Purification and characterization of α_1-antitrypsin secreted by recombinant yeast *Saccharomyces diastaticus*. J Biotechnol 1995;42:191–5. http://dx.doi.org/10.1016/0168-1656(95)00079-6.
[12] Arnold LD, Vaishnav P. Production of recombinant proteins by microbes and higher organisms. Biotechnol Adv 2009;27:297–306. http://dx.doi.org/10.1016/j.biotechadv.2009.01.008.
[13] Graf A, Dragosits M, Gasser B, Mattanovich D. Yeast systems biotechnology for the production of heterologous proteins. FEMS Yeast Res 2009;9:335–48. http://dx.doi.org/10.1111/j.1567-1364.2009.00507.x.
[14] Macauley-Patrick S, Fazenda ML, McNeil B, Harvey LM. Heterologous protein production using the *Pichia pastoris* expression system. Yeast 2005;22:249–70. http://dx.doi.org/10.1002/yea.1208.
[15] Buntemeyer H, Tebbe H, Lutkemeyer D, Lehmann J. Rapid high-performance liquid chromatographic quantification of recombinant human antithrombin III during production and purification. J Chromatogr B Biomed Sci Appl 1994;662:209–16. http://dx.doi.org/10.1016/0378-4347(94)00266-5.
[16] Vemula S, Thunuguntla R, Dedaniya A, Kokkiligadda S, Palle C, Ronda SR, et al. Improved production and characterization of recombinant human granulocyte colony stimulating factor from *E. coli* under optimized downstream processes. Protein Expr Purif 2015;108:62–72. http://dx.doi.org/10.1016/j.pep.2015.01.010.
[17] Ohya T, Hayashi T, Kiyama E, Nishii H, Miki H, Kobayashi K, et al. Improved production of recombinant human antithrombin III in Chinese hamster ovary cells by ATF4 overexpression. Biotechnol Bioeng 2008;100:317–24. http://dx.doi.org/10.1002/bit.21758.
[18] Gurramkonda C, Adnan A, Gabel T, Lunsdorf H, Ross A, Nemani SK, et al. Simple high-cell density fed-batch technique for high-level recombinant protein production with *Pichia pastoris*: Application to intracellular production of Hepatitis B surface antigen. Microb Cell Fact 2009;8:13. http://dx.doi.org/10.1186/1475-2859-8-13.
[19] Evans L, Hughes M, Waters J, Cameron J, Dodsworth N, Tooth D, et al. The production, characterisation and enhanced pharmacokinetics of scFv-albumin fusions expressed in *Saccharomyces cerevisiae*. Protein Expr Purif 2010;73:113–24. http://dx.doi.org/10.1016/j.pep.2010.05.009.
[20] Siegel RS, Brierley RA. Methylotrophic yeast *Pichia pastoris* produced in high-cell-density fermentations with high cell yields as vehicle for recombinant protein production. Biotechnol Bioeng 1989;34:403–4. http://dx.doi.org/10.1002/bit.260340315.
[21] Wilken LR, Nikolov ZL. Recovery and purification of plant-made recombinant proteins. Biotechnol Adv 2012;30:419–33. http://dx.doi.org/10.1016/j.biotechadv.2011.07.020.
[22] Liu HF, Ma J, Winter C, Bayer R. Recovery and purification process development for monoclonal antibody production. MAbs 2010;2:480–99. http://dx.doi.org/10.4161/mabs.2.5.12645.
[23] Graslund S, Nordlund P, Weigelt J, Hallberg BM, Bray J, Gileadi O, et al. Protein production and purification. Nat Methods 2008;5:135–46. http://dx.doi.org/10.1038/nmeth.f.202.
[24] Wu S, Lourette NM, Tolić N, Zhao R, Robinson EW, Tolmachev AV, et al. An integrated top-down and bottom-up strategy for broadly characterizing protein isoforms and modifications. J Proteome Res 2009;8:1347–57. http://dx.doi.org/10.1021/pr800720d.
[25] German BV. Predictions of the secondary structure of Antithrombin I11 and the location of the heparin-binding site. J Biol Chem 1984;259:2531–6.